Int. J. Mol. Sci. **2004**, *5*, 239-264

International Journal of
Molecular Sciences
ISSN 1422-0067

www.mdpi.org/ijms/

Molecular Orbital and Density Functional Study of the Formation, Charge Transfer, Bonding and the Conformational Isomerism of the Boron Trifluoride (BF_3) and Ammonia (NH_3) Donor-Acceptor Complex.

Dulal C. Ghosh * and Soma Bhattacharyya

Department of Chemistry, University of Kalyani, Kalyani – 741235, India.

* Author to whom correspondence should be addressed: E-mail: dulal@klyuniv.ernet.in; FAX: (+91) 33-2582 8282.

Received: 15 June 2003; in revised form: 19 September 2004 / Accepted: 20 September 2004 / Published: 30 September 2004

Abstract : The formation of the $F_3B–NH_3$ supermolecule by chemical interaction of its fragment parts, BF_3 and NH_3, and the dynamics of internal rotation about the 'B–N' bond have been studied in terms of parameters provided by the molecular orbital and density functional theories. It is found that the pairs of frontier orbitals of the interacting fragments have matching symmetry and are involved in the charge transfer interaction. The donation process stems from the HOMO of the donor into the LUMO of the acceptor and simultaneously, back donation stems from the HOMO of acceptor into the LUMO of the donor. The density functional computation of chemical activation in the donor and acceptor fragments, associated with the physical process of structural reorganization just prior to the event of chemical reaction, indicates that BF_3 becomes more acidic and NH_3 becomes more basic, compared to their separate equilibrium states. Theoretically it is observed that the chemical reaction event of the formation of the supermolecule from its fragment parts is in accordance with the chemical potential equalization principle of the density functional theory and the electronegativity equalization principle of Sanderson. The energetics of the chemical reaction, the magnitude of the net charge transfer and the energy of the newly formed bond are quite consistent, both internally and with the principle of maximum hardness, PMH. The

dynamics of the internal rotation of one part with respect to the other part of the supermolecule about the 'B–N' bond mimics the pattern of the conformational isomerism of the isostructural ethane molecule. It is also observed that the dynamics and evolution of molecular conformations as a function of dihedral angles is also in accordance with the principle of maximum hardness, PMH. Quite consistent with spectroscopic predictions, the height of the molecule's barrier to internal rotation is very small. A rationale for the low height of the barrier has been put forward in terms of the energy partitioning analysis. On the question of origin of the barrier to internal rotation, we conclude that the conformational barrier to internal rotation does not originate from a particular region of the molecule, but rather it is a result of the subtle conjoint interplay of a number of opposing effects of one- and two-center bonded and nonbonded energy terms involving the entire skeleton of the molecule.

Keywords: Charge transfer, chemical potential equalization, conformational isomerism and maximum hardness principle, barrier to internal rotation.

Introduction

Boron trifluoride, BF_3, is a Lewis acid [1] and in Pearson's HSAB classification [2] it is a hard acid. It is widely known that the BX_3 molecules (X=H, or halogen atom) form stable and well defined supermolecular adducts with a large number of Lewis bases [1] that are classified as non-metallic boron-coordination [3] compounds. In fact, the adduct of BF_3 with NH_3 was the first known coordination compound of any element [4]. Lewis classified this important class of adduct molecules as electron pair donor-acceptor complexes [1]. Haaland [5] defined the new boron–ligand (B–L) bond as a dative bond in view of the fact that the dissociation of donor-acceptor complexes always yields two closed shell fragments, of which one is an electron pair donor and the other is an electron pair acceptor. It may be pointed out that the energy of the newly formed bond is pivotal for the energetics of the donor-acceptor complex formation. The characteristic structural feature exhibited by the BF_3 system in chemical reactions is that it reorganizes from a planar (D_{3h}) to a pyramidal (C_{3v}) shape prior to the actual chemical reaction event. It is also observed that donors, in turn, may reorganize in order to participate in the chemical event, but the reorganization in these donors is usually very small. Ghosh *et al*. [6,7] have recently suggested an intuitive description of the structure and dynamics of the physical process of D_{3h} to C_{3v} reorganization of BF_3 type molecules prior to the event of chemical reaction with donors, according to the scheme depicted in Figure1. Ghosh *et al.* [7] have also performed a comparative frontier orbital and density functional study of the variation of stability and reactivity of BF_3 and BH_3 molecules associated with their physical process of D_{3h} to C_{3v} structural reorganization prior to a chemical reaction event according to Figure 1 and have concluded that the hardness or softness is not an invariable static property but rather a dynamic variable property of the molecules.

The findings of this study further conclude that the event of structural reorganization according to Figure 1 not only makes the molecules intrinsically more reactive, but also the relative order of their reactivity in the equilibrium state may be reversed.

Figure 1. The intuitive structure and dynamics of the structural reorganization prior to the event of chemical reaction of BX_3 with the donor (L) molecules.

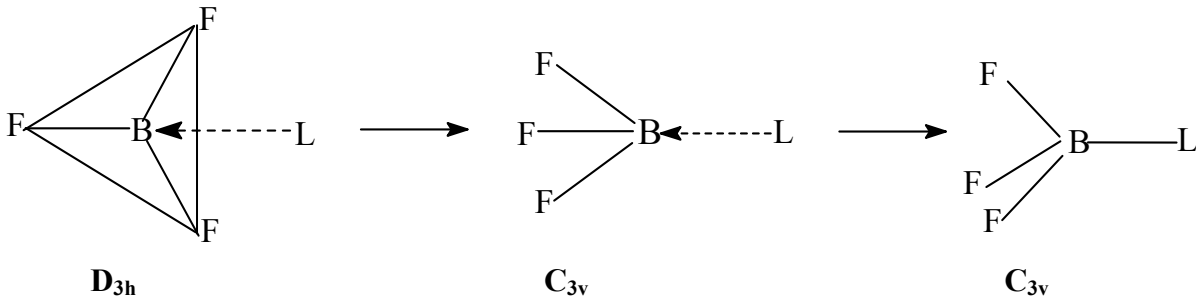

D_{3h} **C_{3v}** **C_{3v}**

The $F_3B–NH_3$ supermolecule, formed by the charge transfer interaction between BF_3 and NH_3, is isostructural with ethane ($H_3C–CH_3$) and ammonia-borane ($H_3B–NH_3$). One part of the supermolecule swings by torsion with respect to the other part about the newly formed 'B–N' bond, thereby generating an infinite number of conformational isomers between two extreme conformers – staggered and eclipsed. The physical process of charge transfer associated with the donor-acceptor interaction leading to the formation of the adduct supermolecule is controlled by the symmetry of the frontier molecular orbitals [8] and the electronegativity difference of the interacting fragments [9]. The origin of charge transfers and mechanism of interaction of molecular orbitals, MO's, of donor and acceptor fragments in the interaction become distinct and transparent in the method of analysis of electronic structure of donor-acceptor complexes developed by Fukui [8]. Ghosh [10] has cast this method of elucidation of the mechanism of the donor-acceptor interaction in a simpler form. The results of such theoretical analysis [8,10] reveal that the two frontier orbitals, the highest occupied molecular orbital, HOMO, and the lowest unoccupied molecular orbital, LUMO, of both donor and acceptor systems are principally involved in charge transfer and bonding in the formation of the donor-acceptor complexes. It is revealed that a simultaneous process of donation from the donor HOMO into the acceptor LUMO and back donation from the HOMO of the acceptor into the LUMO of the donor tells the entire story of formation of donor-acceptor complexes [8,10]. Ghosh and Jana [7] have pointed out that in order to initiate the process of charge transfer and bonding between the interacting molecular fragments the respective pairs of the frontier orbitals of both the systems must have matching symmetry. It is further pointed out that such physical process of D_{3h} to C_{3v} reorganization of geometry of BX_3 systems prior to the event of chemical reaction is a symmetry requirement because if the acceptor molecule remains in D_{3h} form, the symmetry species of the HOMO and LUMO pairs of the interacting subsystems are different and the overlap integral between such frontier orbitals vanishes to zero and the charge transfer reaction cannot occur at all.

The magnitude and the driving force of charge transfer between the donor and acceptor fragments could be rationalized in terms of a qualitative generalization known as the electronegativity equalization principle [9] which implies that if two reactants are brought together, electrons will flow from species of lower electronegativity to that of higher electronegativity until the electronegativity of all the systems – the donor, the acceptor and the adduct – become equal at some intermediate value. The qualitative conceptual terms 'hard' and 'soft' and the HSAB principle of Mulliken [11] and Pearson [2] and the electronegativity equalization principle [9] have now been placed on a sound theoretical basis by a density functional treatment [12, 13, 14]. The density functional HSAB principle has been a very useful paradigm for the study of the electronic structure and reactivity of molecules [12,13]. Parr *et al*. [12] and Parr and Pearson [13], using the density functional theory, DFT [14], as a basis have rigorously defined the hardness, η, and proposed a new fundamental quantity, μ, the electronic chemical potential, as a new index of chemical reactivity. Parr *et al.* [12] identified the newly discovered quantity, the chemical potential μ, with the electronegativity (χ) as $\chi = -\mu$. They have also justified the electronegativity equalization principle of Sanderson [9] in terms of the new density functional parameter, μ [12]. Parr, Pearson and others [12,13,15,16] have critically analyzed the role of chemical potential in chemistry and seem to have suggested that the chemical potential provides a new rationale for explaining chemical reactions through the process of charge transfer. This rationale is the principle of chemical potential equalization, which states that the charge transfer occurs from a system of higher chemical potential to system of lower chemical potential till the chemical potential of the donor, the acceptor and the adduct are equal to each other. If we assume A is a Lewis acid and B is a Lewis base, then electrons will flow from B to A to form a coordinate covalent bond between A and B and this can only happen if $\mu_B > \mu_A$. Electron flow will increase μ_A and decrease μ_B until they are equal to each other and to the electronic chemical potential of AB i.e. μ_{AB}.

Another popular structural principle has been the maximum hardness principle PMH of Pearson [17], which can be stated as "there seems to be a rule of nature that molecules arrange themselves so as to be as hard as possible". Parr and Chattaraj [18] have provided a theoretical justification of PMH. A number of further studies [19] have critically analyzed the PMH statement and have also justified it. Chattaraj *et al.* [20] hold that chemical hardness has been a cardinal index of molecular structure, reactivity, binding and dynamics. Since then the global hardness concept has been an index of stability of molecular structures. When the molecule evolves from an unstable form towards a stable equilibrium form its global hardness increases and when the global hardness decreases the molecule evolves from an equilibrium form to a non-equilibrium form. Although the PMH is strictly valid for constant chemical potential, its relaxation is also observed. Pearson and Palke [21] have demonstrated that the operation of PMH is fulfilled by the structural situation associated with the formation of the transition state, T.S, in a chemical reaction, in inversion, asymmetric deformation, internal rotation, and many isomerization reactions.

Ghosh *et al.* [22] suggested that the hardness of an aggregate molecule is the reciprocal of the aggregate softness computed as the average of the softness of the constituent fragments. Datta [23], on the other hand, suggested a geometric mean formula for the same purpose. Gázquez [24], while

correlating the bond energy and the hardness differences and further justifying principle of maximum hardness, PMH [17,18], has pointed out that in practice the energy of the bond between A and B is determined by their hardness difference and the hardness and softness concepts play a fundamental role in the description of chemical events.

Another important aspect to be considered is the rotation dynamics of the $F_3B–NH_3$ supermolecule. One part of the molecule rotates with respect to the other part about the 'B–N' bond and thus leads to the conformational isomerism of the molecule. Knowledge of the dynamics of the structural isomerism is very important because of the fact that the origin and development of the barrier to internal rotation within a molecule is of common interest to theoretical, experimental, and biological chemists [25]. The physical process of generation of *staggered* ⟛ *eclipsed* conformers is in fact a rotational isomerization process whereby the electron density among atoms in a molecule undergoes a continuous reorganization and redistribution, though the total number of electrons is conserved, even though there may be an intramolecular charge transfer process. Such rotational isomerization processes can be addressed in terms of density functional theory, which is firmly based on electron density. The rotational isomerization process, in a theoretical analysis of the physical process, can be followed by the potential functions. The potential functions can be the total energy function or any other suitably defined potential functions.

Recently, density functional theory, DFT, was found to be quite well suited for addressing and describing such physical processes of internal rotation because it provides appropriate theoretical parameters like electronic chemical potential and molecular hardness to study such processes [16,26,27]. The hardness profile is found to be a faithful descriptor of the dynamics of internal rotation of molecules [16,26,27]. The origin of the barrier to internal rotation is an ever-enticing problem of theoretical chemistry. Schleyer *et al*. [28] have pointed out that while quite accurate barrier heights can be calculated, even at relatively modest levels of theory, the origin of barrier is still debatable. However, Ghosh *et al.* [29,30] have observed that the determination of the origin of barrier to the physical process of inversion in terms of energy partitioning analysis of Fischer and Kollmar [31] is a meaningful venture.

A number of reports of study of the electronic structure, binding and formation of $F_3B–NH_3$ have appeared [32-35], but it seems that the study of mechanism of charge transfer interaction has not been taken up by any group. There is no report of any attempt of a density function rationale of charge transfer interaction between BF_3 and NH_3 during the formation of the supermolecule. Also there are no reports of detailed studies of the conformational isomerism of the $F_3B–NH_3$ molecule, although a knowledge of the dynamics of the structural isomerism is very important in correlating the physico-chemical properties and the biological activity of a molecule. Hence, the study of its conformational phenomena is necessary for a better understanding of the structure, stability and reactivity of the $F_3B–NH_3$ molecule. We have, therefore, undertaken the molecular orbital and density functional study of the formation of $F_3B–NH_3$ from its interacting fragments, BF_3 and NH_3 and the conformational isomerism due to dynamics of internal rotation of the molecule.

Method of Computation

1. The Density Functional parameters.

The exact density functional definitions of the chemical potential, μ, and hardness, η, are as follows [12,13]:

$$\mu = (\delta E/\delta N)_V \qquad \eta=1/2(\delta\mu/\delta N)_v \qquad (1)$$

where N is the number of electrons and v is the potential due to the nuclei plus any external potential. The operational and an approximate definition of above quantities are

$$\mu=-(I+A)/2 \qquad \eta=(I-A)/2. \qquad (2)$$

where I is the ionization potential and A is electron affinity of the system
On further approximation, the eqn. (2) takes the form:

$$-\varepsilon_{HOMO} = I \qquad -\varepsilon_{LUMO} = A \qquad (3)$$

$$\eta = (\varepsilon_{LUMO} - \varepsilon_{HOMO})/2 \qquad (4)$$

$$\mu = (\varepsilon_{HOMO} + \varepsilon_{LUMO})/2 \qquad (5)$$

where ε_{LUMO} and ε_{HOMO} are the eigen values of the LUMO and HOMO respectively.

2. Calculation of occupation numbers of the MO's of the interacting fragments after the chemical interaction.

The details of algorithm for the calculation of the occupation numbers are discussed in the original source [8,10] and we only mention here the salient features. Let A, B and AB represent the acceptor, donor and adduct respectively, which have closed shell electronic structures.

Let Φ, Ξ and Ψ be the row vectors that include both the ground state (or occupied) as well as virtual SCF molecular orbitals and constitute n, m and (n+m) orthonormal sets respectively.

$$\mathbf{\Phi} = (\phi_1\phi_2\phi_3.....\phi_n) \qquad (6)$$

$$\mathbf{\Xi} = (\chi_1\chi_2\chi_3.....\chi_m) \qquad (7)$$

$$\mathbf{\Psi} = (\psi_1\psi_2\psi_3.....\psi_{m+n}) \qquad (8)$$

where ϕ_I's , χ_I's and ψ_I's are the MO's of A, B and AB respectively. A and B are kept at the same nuclear configuration as in the adduct AB.

The LCAO expansion of the row vectors can be written as

$$\mathbf{\Phi = F_A C_A} \qquad (9)$$

$$\mathbf{\Xi = F_B C_B} \qquad (10)$$

$$\mathbf{\Psi = F_{AB} C_{AB}} \qquad (11)$$

where $\mathbf{F_A}$, $\mathbf{F_B}$ are the row vectors of the AO's of A and B.

$$\mathbf{F_A} = (f_1^a f_2^a .....f_n^a) \qquad (12)$$

$$\mathbf{F_B} = (f_1^b f_2^b .....f_m^b) \qquad (13)$$

$$\mathbf{F_{AB}} = (f_1^a f_2^a .....f_n^a \mid f_1^b f_2^b .....f_m^b \qquad (14a)$$

$$= (\mathbf{F_A} \mid \mathbf{F_B}) \qquad (14b)$$

$\mathbf{C_A}$, $\mathbf{C_B}$ and $\mathbf{C_{AB}}$ are n×n, m×m and (n+m)×(n+m) matrices of such LCAO expansions.

Now we expand the MO's of A-B in terms of MO's of A and B; let the required expansion be

$$\psi = \chi' \mathbf{D} \qquad (15)$$

where χ' is the row vector of the MO's of A and B and hence is the (m+n)×(m+n) matrix of this expansion:

$$\chi' = (\varphi_1\varphi_2\varphi_3\ldots..\varphi_n\chi_1\chi_2\chi_3\ldots.\chi_m) \qquad (16)$$

where φ's and χ's are the MO's of A and B respectively.

The expansion of χ' in terms of original AO basis may be written as

$$\chi' = \lambda \mathbf{A}. \qquad (17)$$

where $\lambda = (\mathbf{F_A} \mid \mathbf{F_B})$ (18)

and $\mathbf{A} = \begin{bmatrix} \mathbf{C_A} & \mathbf{O} \\ \mathbf{O} & \mathbf{C_B} \end{bmatrix}$ (19)

Putting the expansion of χ' (Eq.17) into eq. (15) we get:

$$\psi = (\mathbf{F_A} \mid \mathbf{F_B})\, \mathbf{AD} \qquad (20)$$

Comparing eqs (11) and (20), the required matrix for the expansion of the MO's of AB in terms of the MO's of A and B is obtained as follows:

$$\mathbf{D} = \mathbf{A^{-1}C_{AB}} \qquad (21)$$

Since the matrices **A** and $\mathbf{C_{AB}}$ are known, **D** can be calculated easily. The occupation numbers of the MO's of fragmental parts after chemical interaction is computed through **D**. The occupation numbers, ν_I for the MO φ_I of **A** is given by

$$\nu_i = 2\sum_{g=1}^{occ} (d_i^{(g)})^2 + 2\sum_{g=1}^{occ}\sum_{k=1}^{m} d_i^{(g)} d_k^{(g)} S_{ik} \qquad (22)$$

where di's are the elements of **D** matrix and g runs through all the occupied MO's of AB and k runs through all the MO's of B, S_{ik} is the overlap integral between the MO's φ_i and χ_k.

3. Calculation of charge transfer and heat of reaction and estimation of the chemical potential and global hardness of the adduct super molecules from the fragments.

Sanderson [9], Ghosh [22], Datta [23] and Gázquez [24] have suggested various expressions for calculating chemical potential, global hardness, charge transfer and reaction energy of the aggregate molecule in terms of its interacting components. We compute the following:

$$\mu_n = -\left(\prod_{i}^{n} |\mu_i|\right)^{1/n}. \qquad (23)$$

where μ_i is the chemical potential of i-*th* fragment and μ_n is the potential of aggregate or adduct and n is the number of isolated fragments.

Ghosh's [22] additivity formula is given by:

$$1/\eta_n^g = 1/n \sum_i^n 1/\eta_i \quad (24)$$

where η_n^g is the hardness of the aggregate, η_i is the hardness of the ith fragments and n is the number of fragments.

Datta's [23] additivity formula is:

$$\eta_n^d = -(\prod_i^n \eta_i)^{1/n} \quad (25)$$

where η_n^d is the hardness of the aggregate, η_i is the hardness of the ith fragments and n is the number of fragments.

According to Gázquez [24], the amount of charge transfer ΔN from donor (of lower electronegativity) to acceptor (of higher electronegativity) and the reaction energy, ΔE_{reac} may be given as

$$\Delta N = (\mu_B - \mu_A)/(\eta_B+\eta_A) . \quad (26)$$

$$\Delta E_{reac} = - \frac{1}{2} (\eta_{AB} - \eta_A - \eta_B) \quad (27)$$

where η_{AB} represents global hardness of adduct A-B and the other quantities are as stated above.

4. Partitioning of total energy into one- and two-center physical components

The energy-partitioning algorithm is briefly discussed below. The details can be found elsewhere [29, 30,31]. The total CNDO energy of a system is:

$$E = \Sigma E_A + \Sigma\Sigma E_{AB} \quad (28)$$

where E_A is monatomic terms and E_{AB} are diatomic terms. The monatomic terms E_A and the diatomic terms E_{AB} can be further broken down into physically meaningful components as follows:

$$E_A = E^U_A + E^J_A + E^K_A \quad (29)$$

where E^U_A , E^J_A and E^K_A are total monatomic orbital energy, electron- electron repulsion energy, and non -classical exchange energy, respectively.

$$E_{AB} = E^R_{AB} + E^V_{AB} + E^J_{AB} + E^K_{AB} + E^N_{AB} \quad (30)$$

where E^R_{AB} , E^V_{AB} , E^J_{AB} , E^K_{AB} , E^N_{AB} are resonance integrals, total potential attraction of all electrons of A in the field of nucleus of B , total electron-electron repulsion, total exchange energy and total nuclear repulsion, respectively.

Although η and μ are rigorously defined in terms of DFT, Pal *et al*. [36] have pointed out that these quantities can not be rigorously obtained using *ab initio* wave function formalisms and the approximate nature of Koopmans theorem is widely known [37], the density functional quantities are inevitably approximate in nature. It is also stated that the density functional quantities are independent of molecular orbital scheme [38]. Ghosh [10,39] has established that if the CNDO/2D formalism is invoked for the calculation of charge rearrangement during donor acceptor interaction, the result is reliable and the trend of charge rearrangement computed through the CNDO/2D method is quite comparable to that of *ab-initio* methods. It is reported [26,40] that Pople's CNDO method [41] can compute accurate conformational isomerism of molecules. The meaningful partitioning of the total

energy of one and two center components is possible in the semi-empirical method of Pople [31,41]. In view of the above we have adopted CNDO/2 method of Pople and co-workers in the present study. However, the charge rearrangement is not computed through CNDO/2 formalism, but through CNDO/2D formalism which is obtained by simply incorporating the Löwdin's [10,39,42] deorthogonalization technique into the CNDO/2 program. Standard parameters [41] and STO basis set have been used; the coulomb and the overlap integrals are computed through the explicit analytical formulae laid down by Roothaan [43].

The N-end of NH_3 approaches the B-end of BF_3 (C_{3v}) along the $C_3(Z)$ axis to give the adduct supermolecule, $F_3B–NH_3$. The staggered form is the minimum energy conformation. The total energy is minimized with respect to all the geometric parameters – bond angles and bond lengths and in the matter of conformational isomerism study we have followed the geometry optimization technique, GOT. The theoretical quantities are evaluated through the explicit formulae laid down above. In order to perform a conformational analysis, one part of the molecule is rotated with respect to the other part about B–N bond (Z-axis) in 10° steps. The results are presented in the tables and extrapolation of data is done wherever felt necessary.

Results and Discussion

The optimized 'B–N' and 'B–F' bond lengths of the adduct molecules are 1.579Å and 1.49Å, respectively, and remain unaltered under internal rotation about the 'B–N' bond. Other parameters are presented in Table 1. The calculated geometric parameters are quite comparable with experimental values [32-35]. Results demonstrate that the 'B–F' bond stretches on formation of the supermolecule.

Table 1. Geometric parameters of $F_3B–NH_3$ system as a function of torsional angles.

Angle of torsion (Degrees)	∠FBF angle (Degrees)	∠HNH angle (Degrees)	N-H length (A^0)
0	111	109.9	1.072
10	111	109.9	1.071
20	111.1	110	1.071
30	111.1	110.1	1.069
40	111.1	110.1	1.068
50	111.2	110.1	1.068
60	111.3	110.1	1.068

Such stretching of the B–F bond of BF_3 upon planar (D_{3h}) to pyramidal (C_{3v}) reorganization of its structure is quite expected due to the resulting elimination of B–F double bond character already observed by Ghosh *et al*. [6] and others [32-35,44]. From Table 2 it is clear that the energy of D_{3h} to C_{3v} reorganization of BF_3 is quite high, consistent with the suggestion that the planar to pyramidal evolution of the molecular shape is associated with the elimination of the π bond between B and F and stretching of B–F bond [6, 32-35,45].

Table 2. The changes in total energy (ΔE), HOMO-LUMO gap[Δ(Δε)] and chemical potential (Δμ) of donor and acceptor moieties associated with the process geometry change prior to complex formation (all in a.u).

BF_3			NH_3		
ΔE	Δ(Δε)	Δμ	ΔE	Δ(Δε)	Δμ
0.12742	-0.18166	-0.07667	0.00244	-0.02464	0.00077

The reorganization in the NH_3 moiety before the adduct formation is insignificantly small. However, when we compare the sum of the reorganization energy of BF_3 and NH_3 fragments (0.1298627 a.u.) and the energy of the newly formed B–N bond (–0.78367 a.u.), it is evident that the energy of the B–N bond greatly overcompensates the sum of the reorganization energies in the donor and acceptor units. Since the 'B–N' bond energy is pivotal in the energetics of formation and conformational preference of the supermolecule, it is pertinent to note the variation of the energy of the bond as a function of internal rotation. The variation of the 'B–N' bond energy as a function of torsional angle and a rationale of such variation in terms of its physical components are transparent from Table 8. Thus one may conclude that the formation of the F_3B-NH_3 molecule from its constituent fragments in any conformation is quite spontaneous.

The density functional study of the effect of structural reorganization of the acceptor and donor moieties; activation in BF_3 due to structural reorganization.

We know that the HOMO-LUMO gap and the global hardness are the index of chemical reactivity and the chemical potential measures the electron-escaping tendency from a molecule. From Table 2 we see that, due to the D_{3h} to C_{3v} reorganization prior to the event of chemical reaction, the changes in the HOMO-LUMO gap, the global hardness and the chemical potential of BF_3 molecule are -0.18166, -0.09083 and -0.07667 respectively. The characteristic chemical activity of BF_3 molecule is its Lewis acidity. The changes in the density functional parameters demonstrate that the physical process of structural evolution of BF_3 molecule prior to adduct formation increases its chemical reactivity and makes the system more electron-greedy.

Effect of Reorganization in NH_3.

The computed data (Table 2) shows that the reorganization in the donor moiety is small. The changes in the HOMO-LUMO gap, global hardness, and the chemical potential of NH_3 molecule due to the structural reorganization prior to the formation of the adduct are -0.02464, -0.01233, and 0.00077, respectively. Hence the computed density functional data demonstrate that the donor moiety, NH_3, becomes chemically more reactive and more electron donating through the physical process of the structural reorganization before the chemical reaction event. The sharp contrast between the nature of changes in the chemical potential data of the two systems is noteworthy. The BF_3 becomes more acidic or electron-greedy whereas the NH_3 becomes more electron donating or basic through the physical process of structural reorganization preceding the chemical reaction.

The Density Functional Correlation of the process of adduct formation

Table 3 lists the hardness, chemical potential of the donor and the acceptor in the equilibrium state, and that of the adduct molecule. It becomes at once evident from Table 3 that the chemical potential of BF_3 is smaller and that of NH_3 is higher and that of the adduct molecule is in between the chemical potential of donor and acceptor. This simply implies that electronegativity of BF_3 is larger and that of NH_3 is smaller and that of the adduct molecule is in between the electronegativity of the donor and the acceptor. The electronegativity of F_3B-NH_3 evaluated from Sanderson's formula (eqn. 23) is 0.2348 a.u., while its density functional value is 0.2510 a.u. Thus, the formation of the coordination complex F_3B-NH_3 from its constituent fragments BF_3 and NH_3 is in accordance with chemical potential equalization principle of Parr *et al.* [12] and electronegativity equalization principle of Sanderson [9]. The global hardness of the 'aggregate' (i.e. the adduct super molecule) calculated from the hardness values of isolated fragments in terms of additivity formulae of Ghosh (eqn.24) and Datta (eqn.25) are 0.39156 and 0.39336. The corresponding global hardness calculated from DFT is 0.35506. The three values are thus nearly equal to each other.

Table 3. Global hardness (η), Chemical potential (μ) of BF_3, NH_3 and F_3B–NH_3 and charge transfer (ΔN) and reaction energy (ΔE) (all in a.u).

Species	η	μ	$\Delta N = (\mu_B - \mu_A)/(\eta_B + \eta_A)$	$\eta_{AB} - \eta_A - \eta_B$	$\Delta E_{reac} = -½ (\eta_{AB} - \eta_A - \eta_B)$
BF_3	0.35741	-0.36137	(-0.15257+0.36137)/	(0.35506 – 0.35741	0.21764
NH_3	0.43293	-0.15257	(0.43293+0.35741)	– 0.43293)	
F_3B– NH_3	0.35506	-0.25105	= 0.264178	= – 0.43528	

Charge transfer and binding

Having found that the formation of the F_3B-NH_3 adduct molecule from its constituent fragments is quite a spontaneous chemical process from the standpoint of the energetics and the dynamics of the density functional parameters, we now discuss the mechanism of charge transfer and rearrangement during the donor-acceptor interaction between the fragments. Parr and Pearson [13] and Pearson [45] pointed out that the amount of charge transfer is controlled by electronegativity difference between the donor and the acceptor.

Table 4. Occupation Numbers (ν_i) of the molecular orbital, MO's of BF_3 and NH_3 fragments and amount of net transfer of charge due to their interaction .

BF_3			NH_3		
MO's	Eigen value	ν_i	MO's	Eigen value	ν_i
$1a_1$	-1.75077	1.9970	$1a_1$	-1.30916	1.9399
1e	-1.67425	1.9997	1e	-0.73008	1.9791
2e	-1.67425	1.9997	2e	-0.73008	1.9791
$2a_1$	-0.90879	1.9998	$2a_1$	-0.58551	1.7394
3e	-0.87371	1.9989	$3a_1^*$	0.28036	0.0128
4e	-0.87371	1.9989	$3e^*$	0.32922	0.0102
$3a_1$	-0.83915	1.9355	$4e^*$	0.32922	0.0102
$4a_1$	-0.77162	1.9999			
5e	-0.75533	1.9992			
6e	-0.75533	1.9992			
7e	-0.71878	1.9988			
8e	-0.71878	1.9988			
$5a_1^*$	-0.00395	0.3688			
$6a_1^*$	0.21206	0.0068			
$9e^*$	0.27557	0.0141			
$10e^*$	0.27557	0.0141			
	Total	24.3292		Total	7.6707
		(+0.3292)			(–0.3293)

The occupation numbers of the all molecular orbitals of the systems were either 2 or 0 before chemical interaction and all the molecular orbitals which were empty before reaction are marked with asterisks.

It is further pointed out that the energy gap between such interacting orbitals is one of the parameters that control the amount of the net transfer of charge in the donor-acceptor interaction [7,46,47]. The difference of energies of the LUMO of the acceptor and the HOMO of the donor and the HOMO of the acceptor and the LUMO of the donor are of prime importance. The method of theoretical evaluation of charge rearrangement and transfer visualizes that initially the donor and acceptor structurally reorganize as in the adduct and then begin to react chemically by the process of charge transfer. The mutual chemical perturbation may lead to some intramolecular charge rearrangement in each fragment. Hence charge rearrangement and transfer must be both intra- and intermolecular. Table 4 shows some revealing features. We see from this Table that the charge is principally donated from $2a_1$ MO of NH_3 into the $5a_1^*$ MO of BF_3. Incidentally, $2a_1$ is the highest occupied molecular orbital (HOMO) of NH_3 and $5a_1^*$ is the lowest unoccupied molecular orbital (LUMO) of BF_3. It becomes further evident from table that some amount of charge is transferred back from 4e, 5e MOs of BF_3 to $3e^*$, $4e^*$ MOs of NH_3 and it is to be noted that 4e, 5e are the HOMO of BF_3 and $3e^*$, $4e^*$ are LUMO of NH_3.

Thus the charge transfer stems from the HOMO of the donor into the LUMO of the acceptor during the donation process and simultaneously, the back-donation stems from the HOMO of the acceptor into the LUMO of the donor. However, looking at the balance sheet we see that the amount of charge received by $5a_1^*$ (LUMO) of BF_3 is 0.3688 but the depopulation of $2a_1$ (HOMO) of NH_3 is 0.2606. Thus the LUMO of BF_3 has received some charge from other sources. A deeper analysis of the occupation numbers of all the orbitals from Table 4 reveals that although the principally affected orbitals in the charge transfer process are the HOMO of the donor (NH_3) and the LUMO of the acceptor, other orbitals are involved in the process of intra- and intermolecular charge transfer during chemical interaction. Looking at the occupation number of $1a_1$ of the donor we see that this initially doubly occupied MO has lost some charge, a part of which may be placed in $3a_1^*$ in intramolecular rearrangement and partly may be placed in $5a_1^*$ of the acceptor unit because of matching symmetry. On the other hand, $3a_1$ MO of BF_3 has lost a significant amount of charge and this amount must be placed in $5a_1^*$ and $6a_1^*$ in intramolecular rearrangement and $3a_1^*$ of NH_3 in intermolecular rearrangement.

Thus we see although the principal donation and back donation of charge involve the frontier orbitals of the donor and the acceptor and amount of back donation is very small because of the high electronegativity of BF_3 molecule, we have observed some interesting intra- and intermolecular charge rearrangement in present case. Initially occupied σ-type MO $3a_1$ of BF_3 puts some charge to $5a_1^*$ MO of BF_3 (intramolecular) and $3a_1^*$ MO of NH_3 (intermolecular).

The amount of net transfer of charge is quite high. The rationale of the large amount of net transfer of charge may be attempted as follows. The energy gap between the HOMO of the donor and the LUMO of the acceptor is 0.5816 a.u. and that between the HOMO of acceptor and the LUMO of the donor is 0.9992 a.u. This data of difference of eigen values of the frontier orbitals predict that the charge transfer via donation should be much larger than that by back-donation. As a rationale of large net transfer of charge it may be pointed out that the transfer of charge by back donation is small

because of the high energy gap between the orbitals involved in back-donation process and the large electronegativity of BF_3 system .

Correlation of charge transfer and bond formation in terms of DFT parameters

It is evident from Table 3 that the chemical potential difference of the donor and acceptor is considerably smaller than the hardness difference. It is also evident that the amount of charge transfer computed from hardness sum and chemical potential difference is positive and reaction energy is positive. It is also to be noted that the difference of the hardness value of the product and sum of the values of the reactants become negative and accordingly, the reaction energy computed through equn.26 is positive. Thus the change in global hardness and chemical potential in this reaction is in perfect accordance with the maximum hardness principle and bond energies and hardness difference correlation of Gázquez [24].

Conformational analysis of $F_3B–NH_3$

The optimized structural parameters as a function of torsional angles are presented in Table 1. Looking at the potential energy diagram in Figure 2 it becomes at once evident that the pattern of the conformational behavior of $F_3B–NH_3$ and the isostructural ethane [26,48,49] under internal rotation around single bond are similar. The staggered form is minimum energy conformation and most likely the equilibrium form of the molecule, and the eclipsed form is the highest energy conformation. Now, the height of the barrier to the internal rotation about 'B-N' bond at zero vibration level is 0.73 kcal/mole (3.04 kJ/mole). Thus, the height of the barrier is negligibly small and the rotation about the 'B–N' bond is almost free.

Figure 2. Plot of total energy of F_3B-NH_3 system as a function of torsional angles (E-Eclipsed, S-Staggered)

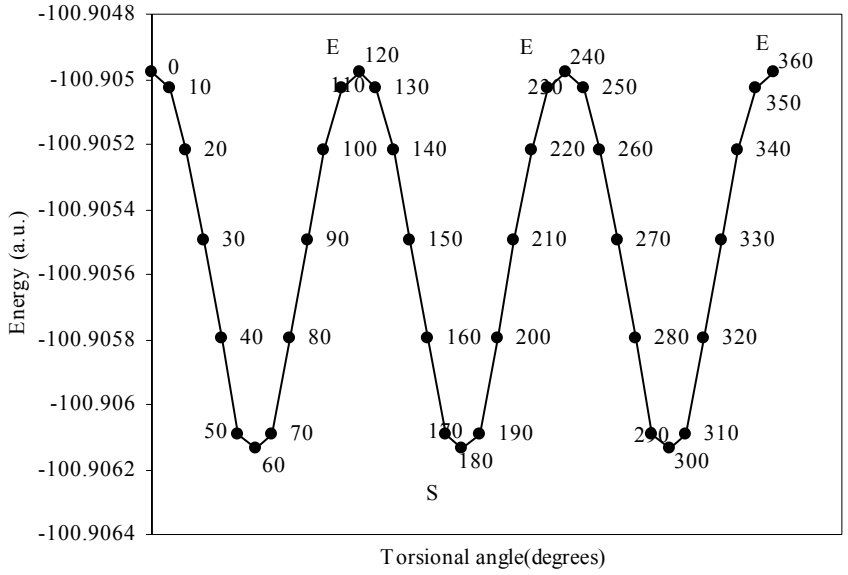

That the height of the barrier to the internal rotation in the donor-acceptor complex formed between NH_3 and BF_3 would be very small was predicted by Legon and Warner [33], in the course of their study of the microwave spectrum of rotational transition in the molecule. Now let us consider the pattern of organization and reorganization of charge density within the molecule under the dynamics of internal rotation of the molecule because, the pattern of charge density reorganization with the evolution of molecular conformation has a significant role on the origin and the development of the height of the barrier to internal rotation. Table 5 and Figures 3 and 4 demonstrate that, as the molecule evolves from an equilibrium staggered form to a non-equilibrium eclipsed form, the charge density variation on the various atoms have two distinct different trends: i) the charge densities on 'N' and 'F' increase monotonically, and ii) that on 'H' and 'B' atoms decrease monotonically.

Table 5. Total energy and gross atomic charge density on different centers as a function of torsional angles (all in a.u.).

Angle of torsion (degrees)	Total Energy	Charge density on B atom	Charge density on N atom	Charge density on H atom	Charge density on F atom
0	-100.90498	2.47328	5.11559	0.80166	7.3353
10	-100.905	2.47337	5.1153	0.80178	7.3353
20	-100.9052	2.47367	5.11483	0.80194	7.33519
30	-100.9055	2.47408	5.11420	0.80210	7.33511
40	-100.9058	2.47418	5.11305	0.80247	7.33500
50	-100.9061	2.47433	5.11222	0.80280	7.33492
60	-100.9061	2.47441	5.11194	0.80298	7.33487

Figure 3. Plot of gross atomic charge densities on N and H atoms in F3B-NH3 system as a function of torsional angles

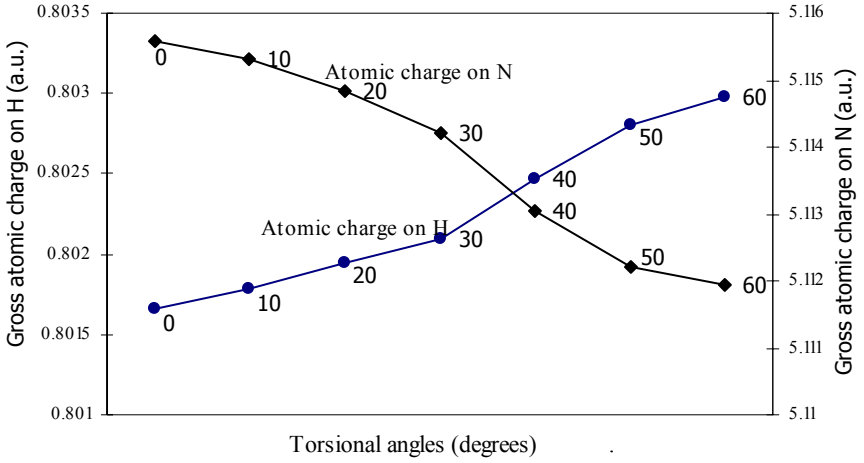

Figure 4. Plot of gross atomic charge densities on B and F atoms of F_3B-NH_3 system as a function of torsional angles

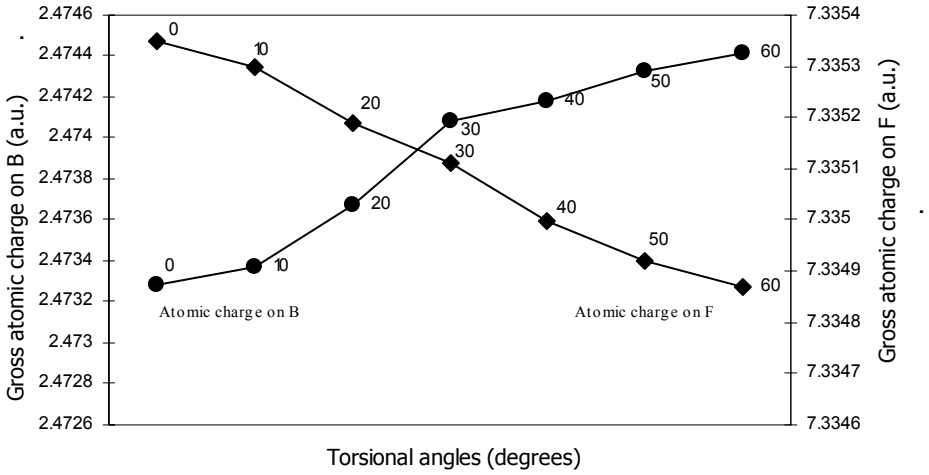

Density Functional study of conformational isomerism

We have calculated the global hardness, η, of the molecule as a function of torsional angles and the ,data are presented in Table 6 and plotted in Figure 5 as a function of torsional angles. A close look at Figure 2 vis-à-vis Figure 5 reveals that the profiles of the global hardness and total energy are mutually homomorphic. In the staggered or minimum energy form of the molecule, the global hardness is maximum, while in the eclipsed or the maximum energy form, the value of hardness is minimum and the curve joining these two extreme points is smooth and continuous. Figure 5 shows that the hardness profile is quite suitable to monitor the process of rotational isomerization in this ethane like molecule. It is also revealed that the physical process of evolution of conformations of the molecule under internal rotation about the 'B–N' bond is perfectly in accordance with the maximum hardness principle [18-20].

Table 6. The Global hardness (η) and chemical potential (μ)as a function of torsional angles (all in a.u.)

Angle of torsion (degrees)	Global hardness	Chemical potential
0	0.3544	-0.25084
10	0.35456	-0.25067
20	0.35466	-0.25094
0	0.35476	-0.25081
40	0.35484	-0.25079
50	0.35493	-0.25096
60	0.35506	-0.25105

Figure 5. Plot of Global hardness of F_3B-NH_3 system as a function of torsional angles (E-Eclipsed, S-Staggered)

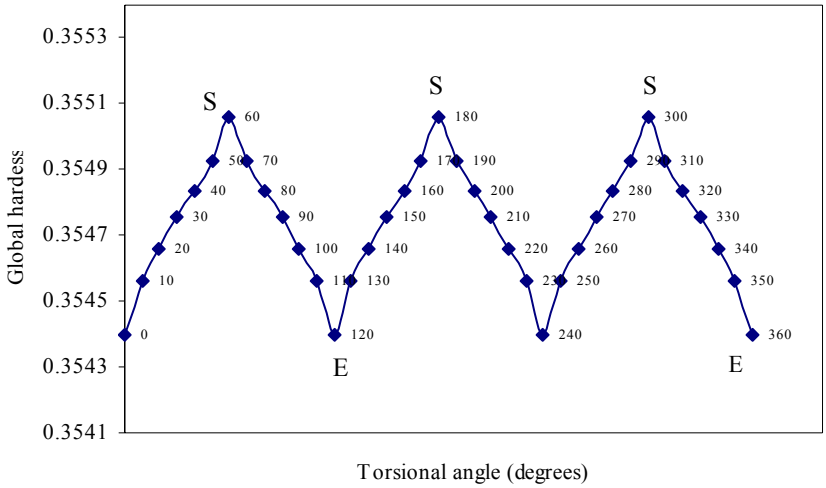

The quest of locating the origin and development of the barrier.

The nature of the evolution of the total energy of the molecule as a function of torsional angles is depicted in Figure 2. Since the barrier height to internal rotation is the difference of energy between the eclipsed and the staggered forms, the nature of the evolution of the one- and two-center energetic effects with the torsional angles may help in the quest of locating the origin and development of the barrier. From the structural formula of the supermolecule it is transparent that there are the following two–center and one-center energy terms:- (i) three bonded interactions– 'B–N', 'B–F' and 'N–H'; (ii) three vicinal non-bonded interactions–'B···H','N···F' and 'H···F'; (iii) two geminal non-bonded interactions – 'H···H' and 'F···F'; (iv) four one-center energy terms- on the 'B','F'.'N' and 'H' atoms. The computed one-center, two-center bonded and non-bonded energies as a function of torsional angle are shown in Tables 7–10**.** We shall first follow how various components of energy evolve when the molecular structure oscillates between two extreme conformations.

Table 7. Two-center bonded interaction energy (a.u.) as a function of torsional angles.

Angle of torsion (degrees)	E(B-F)	E(N-H)	E(B-N)
0	-0.90155	-0.73435	-0.7858
10	-0.901558	-0.73445	-0.7856
20	-0.90158	-0.73453	-0.78509
30	-0.90164	-0.7348	-0.78454
40	-0.90168	-0.73491	-0.78429
50	-0.90179	-0.73493	-0.78397
60	-0.90184	-0.73494	-0.78367

Table 8. 'B–N' bond energy and its physical components (a.u.) as a function of torsional angles.

Angle of torsion (degrees)	(E^J)	(E^N)	(E^V)	(E^K)	(E^R)	E (B-N)
0	4.05983	5.02692	-8.89252	-0.11023	-0.86979	-0.7858
10	4.05975	5.02692	-8.89238	-0.1102	-0.86968	-0.7856
20	4.05986	5.02692	-8.89241	-0.11013	-0.86933	-0.78509
30	4.06004	5.02692	-8.89246	-0.11005	-0.86899	-0.78454
40	4.05979	5.02692	-8.892	-0.11001	-0.86898	-0.78429
50	4.0592	5.02692	-8.89127	-0.10996	-0.86886	-0.78397
60	4.05879	5.02692	-8.89082	-0.10991	-0.86864	-0.78367

Table 9. Two-center non-bonded interaction energy (a.u.) as a function of torsional angles.

Angle of torsion (degrees)	E(N···F)	E(B···H)	E(H···F)	E(F···F)	E(H···H)
0	0.01642	0.00710	-0.01293	0.02635	0.01701
10	0.01638	0.00710	-0.01287	0.02634	0.01701
20	0.01633	0.00692	-0.01279	0.02634	0.01704
30	0.01622	0.0067	-0.01265	0.02632	0.01701
40	0.01605	0.0066	-0.01247	0.02632	0.0171
50	0.01598	0.00656	-0.01236	0.02626	0.01708
60	0.01549	0.00655	-0.01224	0.0262	0.01707

Table 10. One-center energy (a.u) as a function of torsional angles

Angle of torsion (degrees)	E (B)	E (N)	E (H)	E (F)
0	-2.17600	-10.14411	-0.39154	-27.26935
10	-2.17604	-10.14379	-0.39159	-27.26934
20	-2.17688	-10.14351	-0.39164	-27.2693
30	-2.17633	-10.14261	-0.39169	-27.26924
40	-2.17649	-10.14188	-0.39181	-27.26916
50	-2.17652	-10.1416	-0.39193	-27.26907
60	-2.17651	-10.14156	-0.392	-27.26905

A glimpse at Tables 7-10 reveals that as the torsion begins from the eclipsed conformation under internal rotation the bonded, nonbonded two-center and one-center interactions tend to change as follows: (i) the 'B–N' bonded interaction energy increases while the 'B–F' and 'N–H' bonded interaction energies decrease monotonically; (ii) the 'H···H' nonbonded interaction is anomalous while

the 'H···F' and 'B···H', 'N···F' and 'F---F' nonbonded interaction energies maintain a regular trend with torsion, (iii) of the one-center terms, energetic effect on 'B' center is anomalous but it tends to stabilize the staggered form compared to the eclipsed form while that on 'N' and 'F' centers increase and that on 'H' center decreases monotonically. All the energetic effects, except the two anomalous effects stated above, are plotted as a function of torsional angles in Figures 6–12.

Figure 6. Plot of 'B-N' bonded interaction energy of F_3B-NH_3 system as a function of torsional angle.

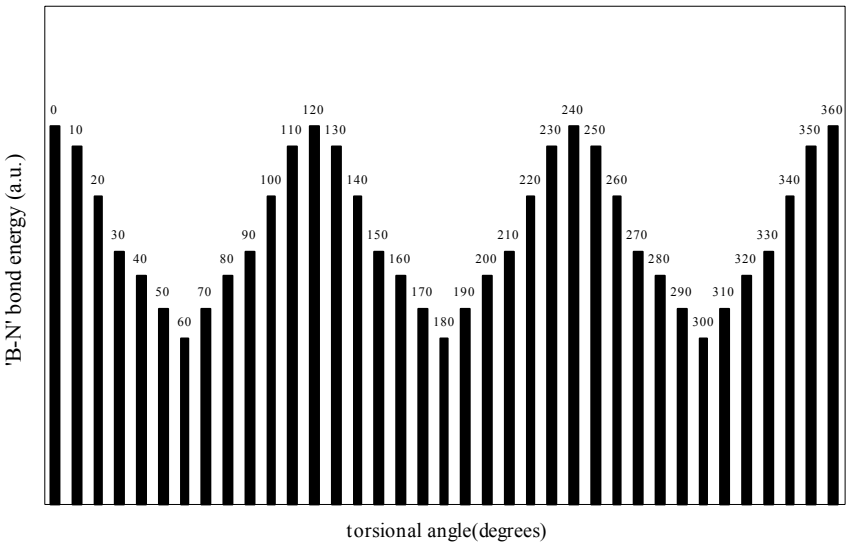

Figure 7. Plot of 'N-H' and 'B-F' two center bonded interaction energies of F_3B-NH_3 system as a function of torsional angle (E-Eclipsed, S-Staggered)

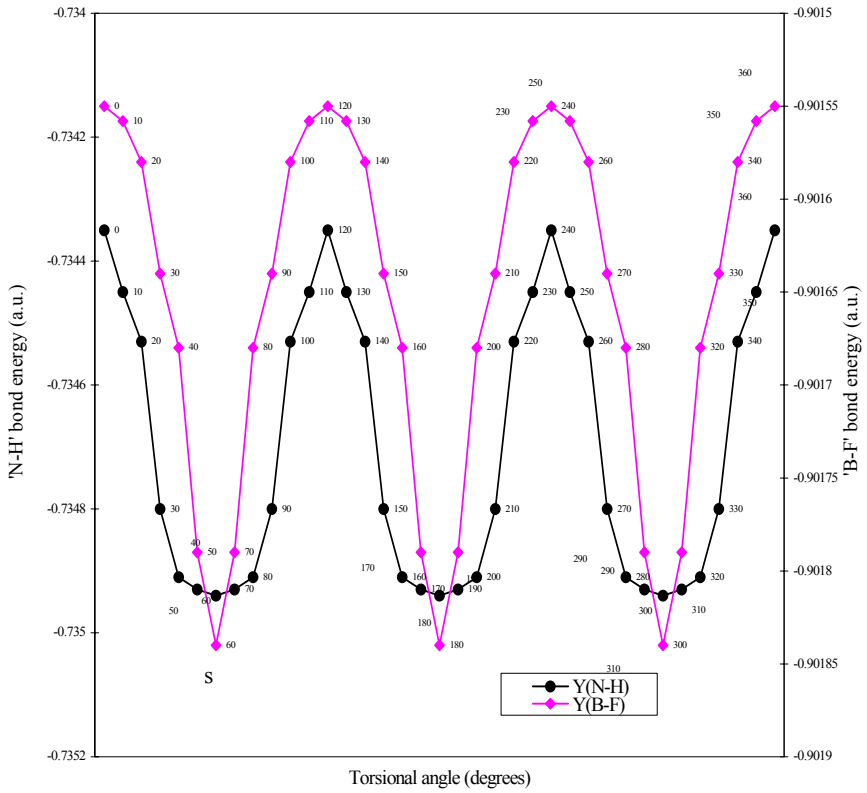

Figure 8. Plot of 'H.···F' non-bonded interaction of F_3B-NH_3 system as a function of torsional angle (E-Eclipsed, S-Staggered)

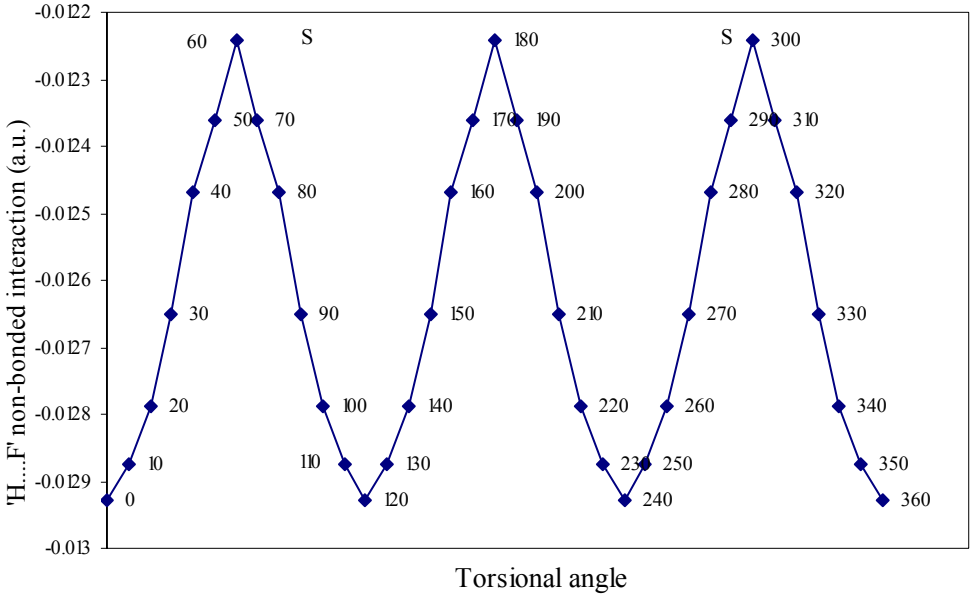

Figure 9. Plot of two-center non-bonded interaction energy of F_3B-NH_3 system as a function of torsional angle.

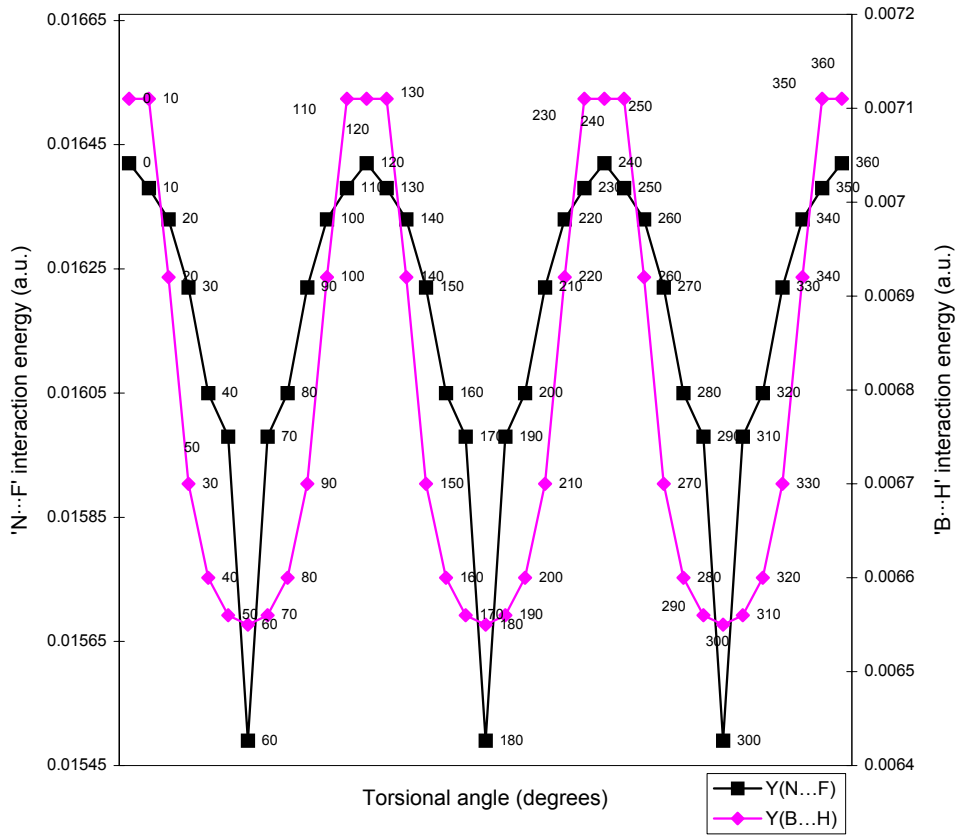

Figure 10. Plot of two-center 'F···F' non-bonded interaction energy of F_3B-NH_3 system as a function of torsional angles (E-Eclipsed, S-Staggered)

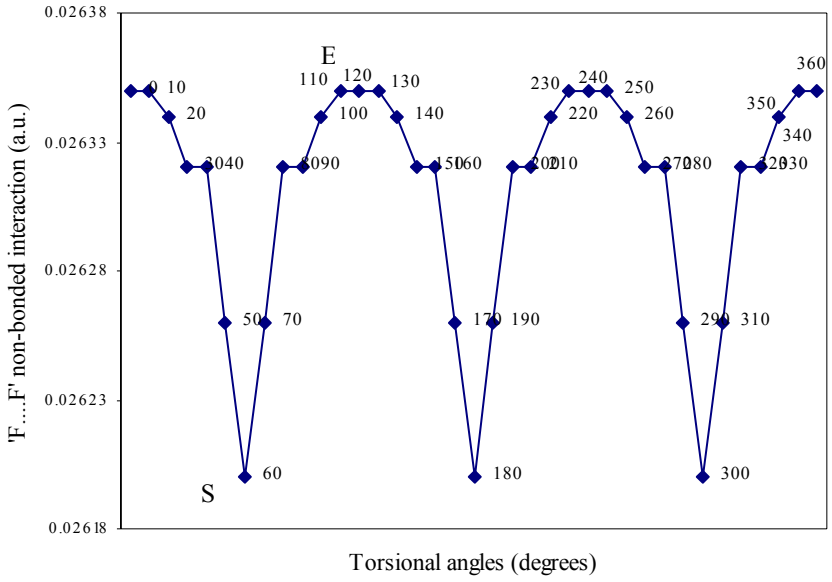

Figure 11. Plot of one-center energy (on N and F) of F_3B-NH_3 system as a function torsional angle (E-Eclipsed, S-Staggered)

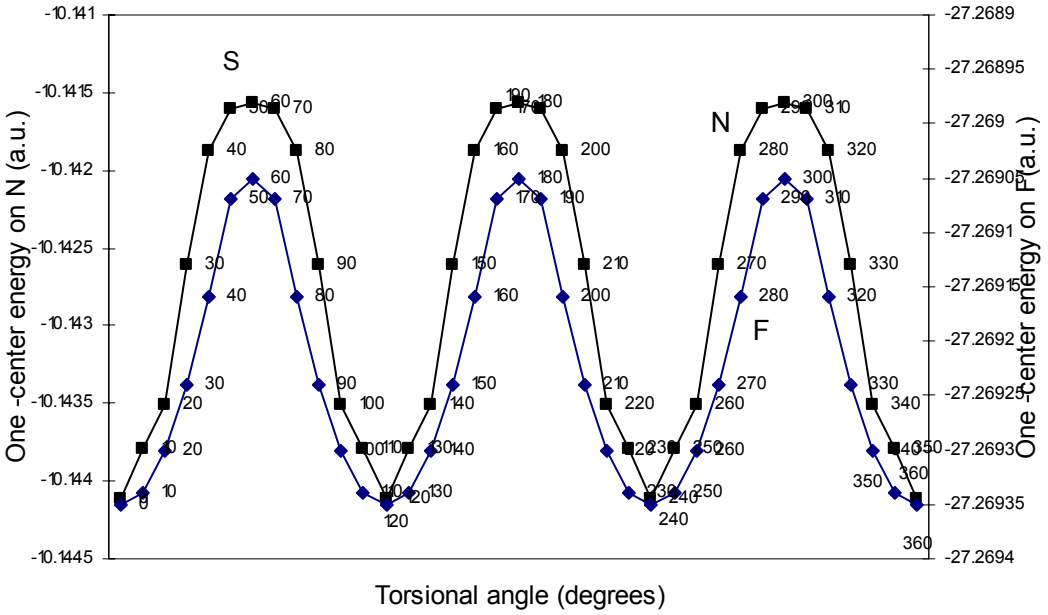

Figure 12. Plot of one-center energy on 'H' of F_3B-NH_3 system as a function of torsional angle.

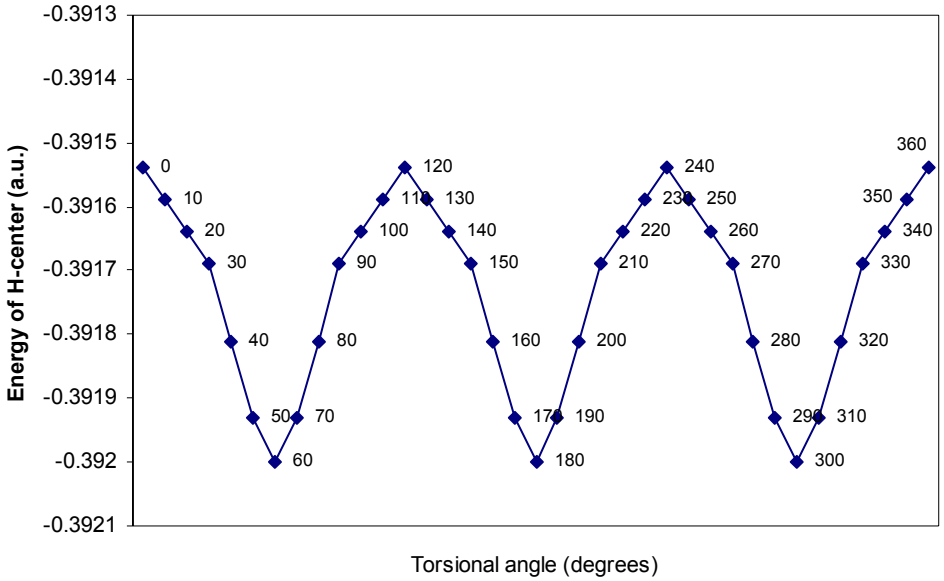

Two-center bonded interactions.

Figures 6 and 7 reveal that the nature of the profiles of the bonded interactions in the F_3B–NH_3 molecule dance to the tune of the conformational behaviour of the molecule under internal rotation. A simple comparison with Figure 2 reveals that all of them can be used as descriptors of the conformational isomerism of the molecule. The 'B–N' bonded interaction tends to stabilize the eclipsed form compared to the staggered form while the other two bonded effects tend to stabilize the staggered form compared to the eclipsed form. Since the barrier height is the difference of energy between the energies of eclipsed and staggered conformations, the 'B–N' bonded interaction tends to decrease the barrier height while the 'B–F' and 'N–H' bonded interactions tend to increase the barrier height.

Two-center nonbonded interactions.

Looking at Table 9 it is evident that the majority of the non-bonded interactions, 'B···H', 'N···F', 'H---H' and 'F---F' are repulsive while only 'H···F' is attractive in all conformations. However, a closer look at table 9 reveals that 'B···H', 'N···F' and 'F---F' favour skewing and staggering and retards eclipsing while "H···F' and 'H---H' favour eclipsing and retards staggering. To have a more clear understanding of the diverse effect of the non-bonded interactions on the conformational behavior of the instant molecule, we have plotted $E_{H\cdots F}$, $E_{B\cdots H}$, $E_{N\cdots F}$ and $E_{F\cdots F}$ terms as a function of torsional angle in Figures 8, 9 and 10 respectively. A comparison of the nature of profiles of Figures 2, 8, 9 10 reveal that Figures 2, 9 and 10 are isomorphic while Figures 2 and 8 are homomorphic having inverse relationship with each other. It is also revealed from the nature of the energy profiles in Figures 8, 9 and 10 that all these nonbonded interactions can be used as a faithful descriptor of the conformational

isomerism of the molecule under internal rotation. The effect of 'B···H', 'N···F' and 'F---F' nonbonded interactions is to accelerate the process of staggering and to retard the process of eclipsing while the other non-bonded interaction, 'H---F' has just the opposite trend because it accelerates the process of eclipsing and retards the process of staggering. The immediate consequence of this differential behaviour of nonbonded interactions upon the rotational barrier is that the 'B···H', 'N···F' and 'F---F' interactions will tend to increase while the 'H···F' and 'H---H' interactions will tend to reduce the magnitude of the height of the barrier.

One–center energy terms.

Now let us consider the variation of one-center energy terms during the process of internal rotation of the molecule. From Table 10 it is evident that one-center energy terms have two distinct opposite effects on the conformational behavior of the molecule. As the molecule evolves from eclipsed to equilibrium form, one-center energy terms on F and N atomic sites increase and that on H decreases monotonically. The energetic effect on the 'B' center is, however, anomalous. On analysis it is found that it tends to stabilize the staggered form compared to the eclipsed form. The one-center effects on the F and N atoms are plotted in Figure 11 while that on the H atom is plotted in Figure 12 respectively. A look at Figures 2, 11 and 12 reveals that Figure 2 and Figure 11 are homomorphic, while Figures 2 and 12 are isomorphic with each other. It is also demonstrated by the nature of the profiles in the figures that the one-center energetic effects on the N, F and H atoms can be used as descriptors of the conformational isomerism of the molecule under internal rotation. Therefore, staggering is favored by one-center energy terms on the B and H atoms and retarded by such energy terms on the F and N atoms.

The rationale for the small height of the barrier to internal rotation.

We have just noted the pattern of variation of all one- and two-center energetic effects along with the total energy change in the F_3B-NH_3 molecule under internal rotation. It is transparent that all the energetic effects do not follow the trend of the total energy change with torsion rather these effects are distinctly divided in to two opposing trends. The barrier height is the result of the complex interplay of two-center bonded and non-bonded interactions and one-center energy terms in the molecule with the evolution of molecular conformations as a function of internal rotation of molecule**.** However, we may venture to put forward a rationale for the small barrier height of the instant molecule in terms of partitioned energy components. We summarize the net effect of each type of interaction. When we consider the effect of one-center interactions we see that the sum of the effects on four different centers is in favor of formation of the staggered form. Hence, the net effect of one-center energy terms tends to increase the magnitude of barrier to internal rotation of the super-molecule. It is also evident from Table 7 that the energy of the 'N-H' and 'B-F' bonds decrease extremely slowly under torsion from eclipsed to staggered form and hence such bonded interactions virtually have no conformational

preference, but the 'B-N' bond favours the physical process of attaining the eclipsed form and retards the development of staggered form. Hence the net effect of bonded interactions seems to prefer the eclipsing process and tends to decrease the barrier height. We have noted above that the entire two-center nonbonded interactions have a pronounced effect on barrier height. Of the nonbonded interactions, the 'N···F' and 'B···H' components favour staggering while the 'H···F' interaction, the most pronounced nonbonded one, favours the eclipsing one. Since any energetic effect stabilizing the eclipsed form reduces barrier height, it transpires that the conjoint action of the 'B–N' bonded and 'H···F' nonbonded interactions make the height of the barrier to internal rotation in the $F_3B–NH_3$ molecule negligibly small. The present study demonstrates that the barrier to internal rotation does not develop from some intramolecular nonbonded interaction.

Conclusions

We have studied the formation of a well-known supermolecule like $F_3B–NH_3$ by the chemical interaction of its interacting donor and acceptor units, BF_3 and NH_3. We have invoked density functional theory and molecular orbital theory to rationalize the formation of the complex and to study the dynamics of the internal rotation of the molecule. It is found that the donor-acceptor interaction is consistent from the standpoint of the energetics of the chemical reaction i.e. the reaction energy, the amount of the net transfer of charge and the energy of the newly formed bond. The process of charge transfer interaction is quite internally consistent from the standpoint of the symmetry of the interacting orbitals, chemical potential and electronegativity equalization principles and maximum hardness principle, MHP. Results demonstrate that the pairs of frontier orbitals on each interacting fragment have matching symmetry and are principally involved in physical process of charge transfer. The process of donation stems from the HOMO of the donor into the LUMO of the acceptor and simultaneously, the process of back donation stems from the HOMO of acceptor into the LUMO of the donor. However, other inner orbitals are also found to be involved in the intramolecular and intermolecular charge rearrangement due to the mutual perturbation of the interacting fragments. The chemical activation computed in terms of the changes in the DFT parameters in the donor and acceptor fragments associated with the structural reorganization just prior to the event of chemical reaction, indicate that BF_3 becomes more acidic and NH_3 becomes more basic just before initiation of chemical reaction. Theoretically, it is observed that the event of the chemical reaction leading to the formation of the supermolecule from its fragmental parts is in accordance with the chemical potential equalization principle of density functional theory and the electronegativity equalization principle of Sanderson because charge is transferred from a species of lower electronegativity and higher chemical potential to another species of higher electronegativity and lower chemical potential and the process is continued till the chemical potential and electronegativity of the donor (NH_3), the acceptor (BF_3), and the adduct ($F_3B–NH_3$) are all equal. The conformational isomerism of the $F_3B–NH_3$ molecule is similar to that of its two structural analogs, ethane and ammonia-borane, and is in accordance with the principle of maximum hardness, PMH. The height of the barrier to internal rotation of the molecule is very small.

A rationale for the small height of the barrier to internal rotation is given in terms of energy partitioning analysis. This analysis has cast some light on the development and origin of barrier to internal rotation. It is once again demonstrated that the barrier does not lie at a particular region of the molecule, but rather it develops from a subtle interplay of one- and two-center energy components within the whole skeleton of the molecule as a function of internal rotation. The case at hand is a remarkable example of the mysterious participation of all the one-center and the two-center bonding and non-bonding interactions to decide the energy barrier. The present study seems to conclude unequivocally that the idea that barrier to internal rotation develops from some intramolecular nonbonded interaction in the molecule is fallacious.

References

1. Lewis, G.N. *Valence and the Structure of Atoms and Molecules*; The Chemical Catalog Company: New York, **1923**.
2. (a) Pearson, R.G. *J. Am. Chem. Soc*. **1963**, *85*, 3533; (b) idem, *Science* **1966**, *151*, 172.
3. Labarre, J.F. *Struct. Bond.* **1978**, *35*, 1.
4. (a) Gay-Lussac, J.L.; Thenard, J.L. *Mem. Phys. Chim. Soc. d'Arcueil* **1809**, *2*, 210; (b) Davy, H. *Phil Trans*. **1812**, *102*, 365
5. (a) Haaland, A. *Angew. Chem*. **1989**, *101*, 1017; (b) idem, *Angew. Chem., Int. Ed. Engl.* **1989**, *28*, 992.
6. Ghosh, D.C.; Jana, J.; Chakraborty, A. *Ind. J. Chem. Soc*. **2002**, *41A*, 462.
7. Ghosh, D.C.; Jana, J. *Int. J. Quant. Chem*. **2003**, *92*, 484.
8. (a) Fujimoto, H.; Kato, S.; Yamabe, S.; Fukui, K. *J. Chem. Phys.* **1974**, *60*, 572; (b) idem *J. Am. Chem. Soc.* **1974**, *96*, 2024.
9. (a) Sanderson, R.T. *Science*, **1951**, *114*, 670; (b) idem, *ibid*, **1952**, *116*, 41; (c) idem, *ibid,* **1955**, *121*, 207; (d) idem, *J. Chem Ed.* **1952**, *29*, 539; (e) idem, *ibid* **1954**, *31*, 238; (f) idem, *Chemical Periodicity*; Reinhold Publishing Corporation: New York, **1960**.
10. Ghosh, D.C. *Indian J. Pure Appl. Phys.* **1984**, *22*, 346; (b) idem, *Indian J. Pure Appl. Phys.* **1989**, *27*,160.
11. Mulliken, R. S. *J. Am. Chem. Soc*. **1952**, *64*, 811.
12. Parr, R.G.; Donnelly, R.A.; Levy, M.; Palke, W.E. *J. Chem. Phys.* **1978**, *68*, 3801.
13. Parr, R.G., Pearson, R.G. *J. Am. Chem. Soc*. **1983**, *105*, 7512.
14. Hohenberg, P.; Kohn, H. *Phys. Rev*. **1964**, *136*, B864.
15. Cedillo, A.; Chattaraj, P.K.; Parr, R.G. *Int. J. Quan. Chem*. **2000**, *77*, 403.
16. Chattaraj, P.K.; Nath, S.; Sannigrahi,A.B. *J. Phys. Chem*, **1994**, *98*, 9143; (b) Sannigrahi, A.B.; Nandi, P.K. *J Mol Struc (THEOCHEM)*, **1994,** *307*, 99.
17. Pearson, R.G. *J. Chem. Ed.* **1987**, *64*, 562.
18. Parr, R.G., Chattaraj, P.K. *J. Am. Chem. Soc.* **1991**, *113*, 1854
19. (a) Pearson, R.G. *Acc. Chem. Res*. **1993**, *26*, 250; (b) Chattaraj, P.K.; Liu, G.H.; Parr, R.G.; *Chem. Phys. Lett*. **1995**, *237*, 171; (c) Ayers, P.W.; Parr, R.G. *J. Am. Chem. Soc.* **2000**, *122*, 2010.

20. Chattaraj, P.K.; Sengupta, S. *J. Phys. Chem.* **1999**, *103*, 6122.
21. Pearson, R.G.; Palke, W.E. *J. Phys. Chem.* **1992**, *96*, 3283.
22. Yang, W.; Lee, C.; Ghosh, S.K. *J. Phys. Chem.* **1985**, *89*, 5413.
23. Datta, D. *J. Phys. Chem. A* **1986**, *90*, 4216.
24. Gázquez, J.L. *J. Phys. Chem.* **1997**, *101*, 9464.
25. Freeman, F.; Tsegai, Z.M.; Kasner, M.L.; Hehre, W.J. *J. Chem. Ed.* **2000**, *77*, 661.
26. Ghosh, D.C. *J. Indian Chem. Soc.* **2002**, *79*, 240.
27. Chattaraj, P.K.; Fuentealba, P. Jaque, P.; Toro, A. *J. Phys. Chem. A* **1999**, *103*, 9307.
28. Schleyer, P.v.R.; Kaup, M.; Hampel, F.; Bremer, M.; Mislow, K. *J Am Chem. Soc.* **1992**, *114*, 6791.
29. Ghosh, D.C.; Jana, J.; Biswas, R. *Int. J. Quantum. Chem*. **2000**, *80*, 1.
30. Ghosh, D.C.; Jana, J.; Bhattacharyya, S. *Int. J. Quantum Chem.* **2002**, *87*, 111.
31. Fischer, H.; Kollmar, H. *Theoret. Chim. Acta*., **1970**, *16*, 163.
32. Jonas, V.; Frenking, G.; Reetz, M.T. *J. Am. Chem. Soc.* **1994,** *116***,** 8741.
33. Legon, A.C.; Warner H.E. *J. Chem. Soc. Chem. Commun*. **1991**, 1397.
34. Dvorak, A.; Ford R.S.; Suenran, R.D.; Levas, F.J.; Leopold., K.R. *J. Am. Chem. Soc.* **1992**, *114* 108.
35. Hoard, J.L.; Geller, S.; Cashin, W.M. *Acta. Cryst.* **1951**, *4*, 396.
36. Ray, R.K.; Chandra, A. K.; Pal, S. *J. Phys. Chem*. **1994**, *98*, 1047.
37. Cederbaum, L.S.; Domeke, W. *Adv. Chem. Phys*. **1977**, *36*, 205.
38. Parr, R.G.; Yang W. *Density Functional Theory of Atoms and Molecules*; Oxford University Press: New York, **1989**.
39. Ghosh, D.C. *Proc. Indian. Acad. Sci.* **1984**, *93* 33.
40. Gordon, M.S. *J. Am. Chem. Soc.* **1969**, *91*, 3122
41. Pople. J.A.; Beveridge D.L. *Approximate Molecular Orbital Theory*; McGraw-Hill: New York, **1970.**
42. Löwdin, P.O. *Adv. Phys. (USA)* **1956**, *5*, 111.
43. Roothaan C.C.J. *J. Chem. Phys*. **1951**, *19*, 1445.
44. Janda K.C.; Bernstein, S.S.; Steed, J. M.; Novick, S.E.; Klemperer, W. *J. Am. Chem. Soc.* **1978,** *100*, 8074.
45. Pearson, R.G. *Inorg. Chem.* **1988**, *27*, 734.
46. Zhou, Z., Parr, R.G. *J. Am. Chem. Soc*. **1990**, *112,* 5720.
47. Parr, R.G., Zhou, Z. *Acc. Chem. Res*., **1993**, *26*, 256.
48. Eliel, E.L., Wilen, S.H. and Mander, L.N.; '*Stereochemistry of Organic Compounds'*; Wiley: New York, **1994**.
49. Nasipuri, D. *Stereochemistry of Organic Compounds*; Wiley Eastern Ltd.: New Delhi, **1994**.